Experimental & Analytical Investigation for Optimization of Disc Brake Heat Dissipation Using CFD

Vikash Kumar Agrawal
Mechanical Engineering Department, Veermata Jijabai Technological Institute

H.P. Khairnar
Mechanical Engineering Department, Veermata Jijabai Technological Institute

https://doi.org/10.5109/6625720

出版情報：Evergreen. 9 (4), pp.1076-1089, 2022-12. 九州大学グリーンテクノロジー研究教育センター
バージョン：

Experimental & Analytical Investigation for Optimization of Disc Brake Heat Dissipation Using CFD

Vikash Kumar Agrawal[1,*], H.P. Khairnar[2,]

[1,2]Mechanical Engineering Department, Veermata Jijabai Technological Institute, Mumbai, 400019, India

*Author to whom correspondence should be addressed:
E-mail: vkagrawal_p18@me.vjti.ac.in

(Received August 24, 2022; Revised October 18, 2022; accepted November 13, 2022).

Abstract: One of a vehicle's most crucial duties is braking. It is critical to design the braking system so that the automobile is still safe when braking. When the brakes are applied, the disc brakes dissipate a heat. The heat dissipation of the brake determines the braking system safety. The present investigation has been intended to estimate the heat dissipation rate of the disc brake; for different proposed disc brake structures using CFD and thermal analysis. The thermal stress has been computed at different load, speed and temperature. The outcome provides essential knowledge of the behavior of the disc airflow, which is critical for comprehending the entire airflow. Both local and global correlations could be established using different visualization techniques. It enables to understand the disc brake thermal stability. The temperature at the interface between pad and disc varies from 36.45°C to 97.8°C as the speed varies from 300 rpm to 1100 rpm and load from 20 N to 80 N. The steady state thermal analysis of a disc rotor was performed in order to evaluate the braking performance of a disc brake under braking conditions. Modelling software has been used to design the brake rotor, and CFD is used to analyse it. It can be reported that numerical, CFD & experimental analysis carried out on the proposed new disc brake design demonstrated optimized heat dissipation.

Keywords: Coefficient of Heat Transfer; Computational Fluid Dynamic; Steady-State Thermal; Static Structural; Mass Transfer Coefficient; Interface Temperature

1. Introduction

Many competitors' vehicle functional requirements limit the brake disc and its surrounding component design for adequate airflow: consider the area, drag coefficient, mass, cost, and entire brake system. Nonetheless, due to the considerable weight, acceleration, and speed of the vehicle, the demand for the disc has increased. The objective of study is evaluate the temperature of the brake pad under different operating conditions and establish the interrelation of parameters like load, speed and temperature. The disc brake is the most common form of a brake. When you use the brakes, friction is formed between the brake pad and the disc. Disc brakes are one hydraulic brake form between the caliper and the wheel hub. The squeezing action occurs when the brakes are applied, and the vehicle comes to a complete stop in Fig.1.

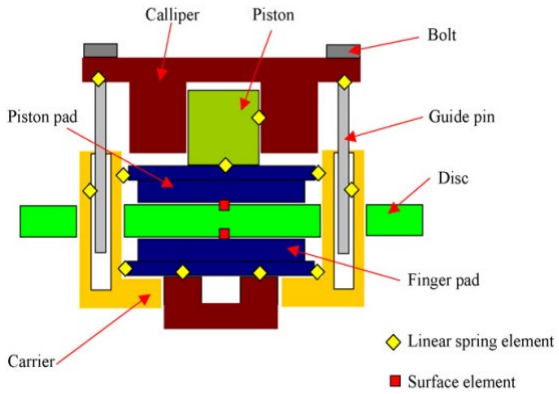

Fig. 1: Contact interaction between disc brake components.

A brake system's primary duty is to slow or stop a vehicle at a reasonable time. As a result, a brake system must be reliable to provide greater control to the operator. The motion of every moving vehicle generates kinetic energy. The higher the vehicle's velocity and kinetic energy, the faster it moves. Computational Fluid Dynamics is a valuable technique for predicting fluid flow heat transport, and mass transfer. It operates on

the principles of energy, mass, and momentum conservation. Temperature, velocity, pressure, density, and other variables are determined using these equations. It can be used to assess design possibilities and, as a result, optimize brake rotor design before prototype component manufacture.

However, whether it's used to forecast temperature rises or levels of thermal stress, there is a problem because the heat loading and convective boundary conditions for a certain braking sequence are not explicitly established. Erroneous results will be produced by inaccuracy in heat inputs and outputs. Analysis error is more pronounced in heat cycles that are long, which show the effects of rising temperatures and the creation of thermal cracks. Mathematical modeling was carried out to estimate the mass transfer coefficient using dimensionless number with pad pressure and disc tightening conditions.

The objective is to attain a high level of system reliability at an affordable price. The safety aspects of automotive technology are becoming increasingly important in the development of modern vehicles. The process of converting kinetic energy to thermal energy, which must then be released as heat, is known as braking. Overheating can lead to braking system failure, which poses a safety risk. Heat dissipation of brake disc gives the thermal stability.

The present study adopted unique approach and obtained brake disc mass transfer and dimensionless number by using both Navier stokes and energy equation it was further used to optimize the boundary conditions and hole combination on the disc to achieve maximum heat dissipation.

2. Literature review

Belhocine et al. investigated and analyzed using ANSYS and multiphysics was used to model the rotor disc temperature distribution during braking. The whole and finite element analysis techniques are used to predict ventilated brake discs [1]. According to Gao and Lin [2], there's a lot of evidence suggesting that contact temperature is a crucial factor in determining the combined impact, speed, and coefficient of friction of the load and other parameters on specific power friction. For example, the frictional couple's materials' physical and durability properties Experiments found that the sliding speed and applied weight increased. The friction coefficient reduced as the disc temperature rose to 300 °C, but it increased with the temperature plummeting over this point. Increased sliding speed and disc temperature were found to increase the wear rate [3].

On the other hand, the vented disc may exacerbate judder issues by creating a disc surrounded by an unequal temperature field because the vented disc's thermal capacity is lower than the solid disc. During repeated braking, the temperature of the vented disc may rise quicker than the temperature of the solid disc [4]. When changing the shape of the vented disc, thermodynamic capability and thermal deformation should be investigated thoroughly. Abdullah and Schlattmann [5] recently published a study that looked at during repeated engagements. In dry friction systems, temperature distribution is essential under various pressure distributions, the clutch disc's temperature field is calculated using the finite element approach. Jerhamre and Christer [6], the entire computational domain's wall function method was applied for the complete vehicle CFD simulations.

The spinning parts, such as the disc brake, wheel, tire, hub cap, and rim, were subjected to rotational boundary conditions. On the calliper and disc walls, the heat transmission coefficient was estimated. This was accomplished using Prostar, the Star-post-processing CD's program[7]. A symmetry boundary constraint was defined for the outer regions of the computing domain. The turbulence intensity in the velocity inlet was set to 0.1 percent, and the turbulent viscosity of the laminar layer was tuned to 200 times that of the surrounding fluid [8]. The experimental values of the convection coefficient of heat transfer correspond well with the CFD results, especially at slower rotating speeds. At the top of the speed scale, the changes become more pronounced, with CFD models estimating a 10% increase in convection heat transfer coefficient at the vehicle's top speed. The findings are also in line with information provided by other sources researchers [9,10]. More research is now being undertaken in order to attain improved precision and incorporate the entire wheel assembly.

The effect of rotating speed on aero thermal performance was studied by More et al. Rotor speed was discovered to have a significant impact on rotor performance. The aerodynamic properties of the airflow through the thermal performance of the rotor passages is highly influenced by and heat dispersion of ventilated brake discs. It has been discovered that as the blade speed increases, the overall heat transfer rate across the channel increases. This is primarily due to the rise in the mass flow rate of the channel [11]. Using ANSYS Multiphysics, A. Belhocine et al. examined and measured the rotor disc temperature distribution during braking action. Finite element modelling techniques, the distribution of warmth over the ventilated brake disc, is predicted. The rotor's critical temperature while taking into account specific aspects such as braking mode, the material used, and disc geometry. The study [12] also determines the heat flow distribution for the two discs. To investigate general axis-symmetric issues in frequency domain elastodynamics, S. V. Tsinopoulos et al. [13] used a quick Fourier transform in conjunction with an advanced boundary element approach (FFT). The issues were characterized by non-axis-symmetric boundary conditions and axis-symmetric geometry.

In the circumferential direction, Complex Fourier series were used to expand boundary quantities. The

difficulty was effectively broken down into a number of problems; the BEM for Fourier boundary quantities was used to tackle these problems, but only the axis-symmetric body's surface generator was discretized. The FFT algorithm used BEM integrations in Quadratic boundary elements were used to achieve Gauss quadrature in the circumferential direction and circumferential quadrature in the generator direction. The analysis of singular integrals was done in a straightforward and exceedingly precise manner. The FFT numerically reversed the Fourier transformed solution, yielding the final result. The approach has a high level of accuracy and efficiency, as illustrated by numerical examples. A two-disc profile and three distinct rotor disc materials were produced using computer-aided engineering tools.

A. Naga Pheneendra et al. investigated during continuous braking, heat generation, and dissipation in a vehicle's solid disc brake. This research aims to look into the temperature distribution and heat dissipation of the disc rotor as it brakes. The temperature distribution on the disc rotor is predicted using a finite element analysis technique, and the critical temperature of the brake rotor disc is determined. The three heat transfer modes examined are conduction, convection, and radiation. The materials discussed were two alternative disc rotor profiles [14,15], Grey Cast Iron, Aluminum Alloy 6262 T-9, and Carbon-Ceramics. Akiro et al. investigated that thermal energy storage and subsequent cooling are frequently an issue for brake disc designers, especially in alpine descent braking and serial fading braking [16]. Uyyuru et al. investigated the brake disc's construction; its surrounding components have primarily relied on empirical knowledge and experience of airflow to and through the disc up to now. As a result, the cooling qualities of the brake system were determined based on temperature changes during braking testing [17].

Solid disc brakes are more expensive than ventilated disc brakes, and a vented disc brake's geometry has been extensively investigated in the industry. In terms of weight, solid disc brakes are heavier than vented disc brakes. Aside from weight, the benefit of its vent hall improves convective heat transmission [18], Kang and Cho explored the effect of disc brake geometry on heat dissipation efficiency. They determined that vented discs disperse heat better than solid discs after braking [19]; after analyzing the following braking, the surface of the brake disc rotor. Ventilated discs are also more controlled when reducing motorbike speed and give adequate torque when braking [20]. Researchers have also linked the air vent shape design to aerodynamic cooling, improving braking effectiveness during braking [21–23]. Aside from that, the cross-section shape significantly impacts braking performance [24, 25].

Abubakar demonstrated that while using new and unworn material friction, the contact area rises, and as wear advances, rough surfaces become smooth and glazed. It has been demonstrated that wear is more likely on the leading edge than on the trailing edge [26]. James et al. discovered that at 4.2 kHz, there is a changing frequency with positive; the kinetic friction coefficient is $\mu_k = 0.4$, and As a result of the experiments [27], this has been determined. A mathematical model for predicting the thermal behavior of a shoe-and-drum brake system was proposed by Naji et al. [28]. Green's function is used for every stopping braking action to solve the model analytically. The thermal behavior of three different braking actions is investigated: stopping activities such as impulse, unit step, and trigonometric. The thermal sensitivity of various materials utilized for the disk–pad interaction in disc braking systems has been studied extensively [29–36].

Gao and Lin [37] provided an analytical method for determining the contact temperature distribution on the working surface of a brake. Fields of the temperature of the solid rotor with permissible thermodynamic boundaries are characterized by the effects of varying relative sliding speeds on the moving heat source utilizing a transient finite element method. According to numerical results, the brake's working characteristics significantly impact the highest contact temperature and the temperature distribution on the surface.

The non-Fourier heat conduction in a semi-infinite body was examined. The heat wave non-Fourier heat conduction model was used for thermal analysis. Thermal conductivity was assumed temperature-dependent, which resulted in a nonlinear equation [42]. The temperature gradient and thermal conductivity compute the heat flux through the interface. The uncertainty in the heat flux computation may be examined by comparing the differences in the calculated values of heat flux for both the hot and cold specimens in the steady-state condition [43]. The aero-thermal environment of a flying test bed has been assessed both from the engineering-based and CFD-based approaches. Computations with the air modeled as perfect gas highlight that vehicle aero heating is more severe than existing reentry vehicles [44].

Vane geometry's impact on disc brake performance For the transient thermal analysis, pillar type vane geometry was compared to straight vane geometry. Because of improved air circulation in straight vanes, the proposed disc brake has more mass and a higher heat transfer coefficient. It was proposed that a curved vane can help improve disc brake performance even more [48]. The thermal behaviour of cross-drilled and solid disc brake rotors during various braking periods. According to the findings, a solid disc brake is superior when the average braking cycle is short, and a cross-drilled disc brake rotor is superior when the average braking cycle is long [49].

The present study, using comparative analysis, evaluated the impact of geometry on brake disc performance. The parameters of investigation were velocity distribution and steady-state thermal temperature.

3. Analytical investigation

The differential equation governs the steady state heat conduction in a three-dimensional heat transfer problem.

3.1 Navier stokes and energy equation

A rotating disc is used to demonstrate heat, mass, and momentum transmission. Heat-transfer mechanism is used to link the experimentally determined mass transfer rate from a rotating disc in an infinite environment under laminar and turbulent conditions. The experimental analog is demonstrated to be effective in removing the challenges of precise heat-transfer coefficient measurements.

The system's mass transfer coefficient on average is defined based on the formula.

$$k_c = \frac{P_{v,s} V}{mRT_s} \qquad (1)$$

In equation (1), vapor pressure $P_{v,s}$ is the pressure at which the temperature reaches saturation T_s which was not measured. The disc surface temperature and the temperature measured by the thermometer differ only by two modest reversal factors, one of which considers the surface drop temperature owing to sublimation cooling. Its temperature is 91.6°C. Another phrase compensates for the temperature differential between the thermometer's temperature of recovery and cylinder surface temperature. This phrase is used to describe a revolving disc.

Disc brakes have evolved over time to be a dependable method of vehicle deceleration and stopping. Disc brake systems have been designed for a variety of applications. The mechanical equivalent of heat states that motion and heat are interchangeable and that a given amount of work will always generate the same amount of heat if the work is completely converted to heat energy.

The heat transfer measurements and the experimental technique utilized in this study generated an average coefficient of transfer of mass and heat. According to the theory, mass and heat transmission coefficients are consistent throughout the laminar flow regime, the whole surface of a revolving disc. The Sherwood number is defined as the convective mass transfer to mass diffusivity ratio. The Nusselt and Sherwood numbers represent the surface effectiveness of heat and mass convection.

The Sherwood number (Sh) is a dimensionless number used in mass-transfer operations. It denotes the ratio of convective mass transfer to diffusive mass transport rate. The convective mass transfer coefficient (k_c) is a function of the geometry of the system as well as the velocity and properties of the fluid. Dimensionless parameters are frequently used to correlate data from convective transfer.

$$Sh = \frac{k_c r}{D_v} = 0.67\, Re^{0.5} \qquad (2)$$

In the case of fluid with a Prandtl number, heat transport is also governed by equation (2) if the Nusselt number is substituted for the Sherwood number. As a ratio of convection to conduction, the Nusselt number indicates energy transfer from the solid surface boundary to the flowing fluid and across its thickness in a normal to the surface direction.

$$Nu = Sh = cRe^{0.5} \qquad (3)$$

Willsaps and Pohlhausen found, for the rotating disc, an accurate solution to the full Navier-Stokes and energy equations (3). Their results can be condensed to the equation when viscous dissipation can be ignored, as in laminar flow. The Nusselt number indicates energy transfer from the solid surface boundary to the flowing fluid and across its thickness in a normal to the surface direction. The fluid characteristics for flow across an arc surface were recently discovered, and the Nusselt number was calculated to better explain the flow's crossing of the boundary between laminar and turbulent flow.

$$Sh = \frac{Re\, Sc\, \beta_m \sqrt{C_{Dr}/2}}{-14 + 5\beta_m Pr + 5\ln(5\beta_m Pr + 1) + \sqrt{\frac{2}{C_{Dr}}}} \qquad (4)$$

$$Nu = \frac{Re\, Sc\, \beta_H \sqrt{C_{Dr}/2}}{-14 + 5\beta_H Pr + 5\ln(5\beta_H Pr + 1) + \sqrt{\frac{2}{C_{Dr}}}} \qquad (5)$$

The turbulent domain's mass and heat transfer coefficients rise as the radius grows. Equations (4) and (5) local values of the Sherwood or Nusselt number can be predicted using a mass, heat, and momentum transit analogy with modifications given by equation (3). Nusselt values of unity indicate that heat dissipation from the surface is evenly distributed between conduction and convection, as seen in laminar flow. The C_{Dr} values for typical passenger cars has dropped from about 0.5 in the 1960's to around 0.3 in the early 1990's, however it appears to be rising again as the demand for large and four wheel drive vehicles increases. The Stanton number is a dimensionless number that compares the amount of heat transferred into a fluid to its thermal capacity. It is employed in the study of heat transfer in forced convection flows.

$$k_c = n\frac{1}{\pi r_o^2}\left[(k_{c_1}\pi r_c^2) + \int_{r_c}^{r_o}(k_{c_t}2\pi r dr)\right] \quad (6)$$

$$St = \frac{Nu}{RePr} \quad (7)$$

$$St = \frac{\beta_H\sqrt{C_{Dr}/2}}{-14 + 5\beta_H Pr + 5\ln(5\beta_H Pr + 1) + \sqrt{\frac{2}{C_{Dr}}}} \quad (8)$$

According to equations (6), (7) & (8), the local values must be merged over the entire disc surface to determine the mass coefficients' average value. The temperature change is directly proportional to the Sherwood number; the occurrence of the peak Sherwood number value is linked to a change in kinematic viscosity. The thermal expansion causes a fluid density to decrease as temperature rises. Lowering the kinematic viscosity of a fluid with a lower density reduces during a frictional flow. The viscosity kinematic effects exceed thermal gradient at a temperature of 100.6°C or higher, lowering the Sh value.

The formula Pr=constant is used to calculate the average value of the mass transfer coefficient during braking. Prandtl number, on the other hand, focuses on the moving fluid and the interaction between it and heat dissipation. Heat must be dissipated by heat transfer during the brake application of a brake, or the brake may overheat and perhaps burn out the lining.

3.2 Material used

Stainless steel is the material employed in disc brakes. Stainless steel is the most common material used to make disc brakes, composites, and other materials. Because of its excellent corrosion resistance, low wear, good Strength, low friction coefficient, and efficiency in terms of heat, stainless steel is employed despite its high cost. The qualities of stainless steel are as follows in Table 1.

Table 1. Properties of stainless steel.

Description	Value
Density	7850 kg m^{-3}
Tensile Strength at its maximum	1470 N m^{-2}
Ultimate yield capacity	1008 N m^{-2}
Temperature conductivity	25 W m^{-1} °K
Thermal expansion coefficient	9.9 µm m^{-1} °C
Capacity for specific heat	460J kg^{-1} °K

4. CAD model of the brake disc rotor

The disc brake is designed and tested with the numerous aspects of the vehicle in mind. The vehicle's mass determines the disc brake design, force, dynamic weight transfer, acceleration, and disc brake assembly to the wheel hub, among other factors.

The disc brake CAD model in Fig. 2 is created using simulation software; thermal, structural, and wheel assembly components are used to develop the disc brake. Since slots are supplied for good heat transfer and weight reduction, this type of disc brake is also known as a slotted disc brake. Both the front and rear wheels of the vehicle are designed similarly. The proportions of the disc brake has been determined by the best heat transfer and the disc brake minimum weight.

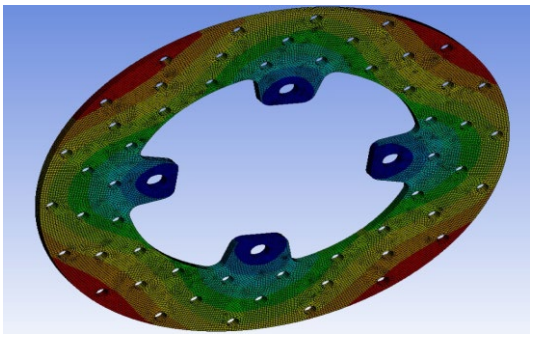

Fig. 2: CAD model of the disc brake.

4.1 Design parameter

The design parameters used in the vehicle's design and analysis are listed below in Table 2. Stainless steel was chosen to create brake discs because it has good thermal conductivity, low noise, low weight, long durability, consistent friction, low wear rate, and a favourable price/benefit ratio. It has a high carbon content and excellent friction, thermal stability, and corrosion resistance summarised in Table 2 and used in this rotor simulation.

Table 2. Design parameters

Description	Value
Mass of the vehicle	1200 kg
Dynamic weight transfer to the rear side	0.5 N
Acceleration of the vehicle	8 m s^{-2}
Vehicle's velocity	12 m s^{-1}
Disc's outside diameter	190 mm
Disc's inside diameter	120 mm
Disc swept area	0.0217 m^2
Effectiveness of brake (a/g)	0.8
Disc's charge distribution factor	0.5

The disc temperature was determined in the initial stage in this investigation. The disc was analyzed in CFD software Ansys Fluent; to achieve this, Fig. 3 indicates the algorithm used for processing.

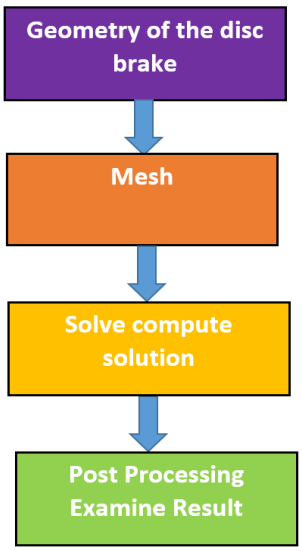

Fig. 3: Numerical methodology for the disc brake using CFD code.

4.2 Boundary conditions

The boundary conditions defined the problems to converge at a single point. These are assumed and estimated based on the problem statement and the experiment's aims. In ANSYS Mechanical, the boundary conditions are determined in Table 3. k-ϵ model have evolved through time. The first time major effort to simulate turbulence in the context of CFD was so called k-ϵ. k is the additional turbulent energy the results from the time fluctuating turbulent motion. Turbulent kinetic energy is a turbulent dissipation (ϵ). In an inlet boundary, the velocity is usually specified by a fixed value condition. The pressure outlet boundary condition defines an outflow condition based on the flow pressure at the outlet.

Table 3. Boundary conditions

Description	Values
Inlet velocity of the air	18 m s^{-1}
Heat transfer coefficient	3570 W m^{-2}
Pressure outlet of the air	1 atm
Inlet temperature of the air	30^0C
Ambient temperature	20^0C
Viscous model	k-ϵ model

4.3 Assumptions

When performing CFD analysis, the following assumptions were used to lessen the complexity of the problem.

1. For the turbulence in the circulation of air around the disc brake, the k-epsilon turbulent model is used.
2. The air input velocity around the brake remains at 18 m/s.
3. In two forms of this simulation, In the interior and outer faces of the brake disc, heat transfer via conduction and convection is significant, resulting in low radiation exchanges. There are no heat dissipation losses.
4. At the specified temperature, the characteristics of air stay the same.
5. The airflow is consistent.

4.4 CFD analysis

Studying a model's static structural and thermal behavior by linking static structural and steady-state thermal analysis is known as structural-thermal analysis. This approach determines the disc brake's stress at constant temperature induced by the thermal load. The disc brake's CAD model is imported into the ANSYS Design Modeler. The disc brake's surface is separated into different portions based on the application of forces. The amount of heat that enters the disc brake and the starting temperature on the disc brake's surface represents the heat energy input to the disc brake. The surface heat transfer is calculated using the results of a CFD analysis, which is used as an input for convection. The disc brake's heat transmission and thermal stress were calculated using these boundary conditions. The outcome of the steady-state thermal study is fed into a static structural analysis tool. In order to execute the static structural analysis, the thermal stress imported are employed as thermal load. The fixed disc brake supports are provided, and the investigation is completed. This method determines the deformation of the disc brake under these conditions as well as the safety factor. The heat transfer coefficient is calculated in the techniques that follow. In the ANSYS Design Modeler, build an air domain around the disc. This air domain has a lot of significance. The heat transfer coefficient is calculated by circulating air around the rotor. When using the solver, air should be created virtually. The enclosures are employed to generate the rotor's air domain. The enclosure's dimensions are as follows:-

Length - 300 mm

Breadth - 300 mm

Height - 300 mm

The dimensions shown above have been calculated iteratively depending on the disc's design. For example, if the enclosure is too tiny, the fluid (air) will cause backflow before the outlet zone. The size of the section will increase the size of the problem, which will increase the time it takes to solve the problem. In ANSYS Mechanical, the boundary conditions for this domain are constructed. The air domain, input, and outflow

conditions of the analysis are depicted in Fig. 4.

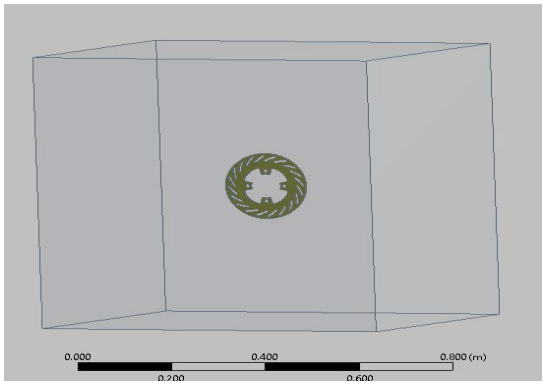

Fig. 4: Box domain.

4.5 Meshing

Meshing before solving the system it is necessary to define the mesh size and mesh type to get the most approximate result. The mesh quality was checked before every analysis and was found to be suitable for the analysis. The orthogonal quality of the mesh obtained was within the required parameters. The mesh quality used is good because the minimum quality was above 0.1 and average quality was near to 0.85. In table 4, the mesh statistics are as follows:

Table 4. Meshing Statistics

Description	Values
Element	657736
Nodes	120872
Orthogonal quality	0.8546
Skewness	0.229367

The mesh details are; Fig.5 settings results after applying boundary conditions and meshing the system is solved. The meshing has been done in ANSYS Mechanical in Fig. 5. The model's element size is estimated to be 2 mm tetrahedrons. Therefore, it is critical to have high-quality mesh to get accurate outcomes. Adopting proximity and curvature functions produces excellent mesh quality.

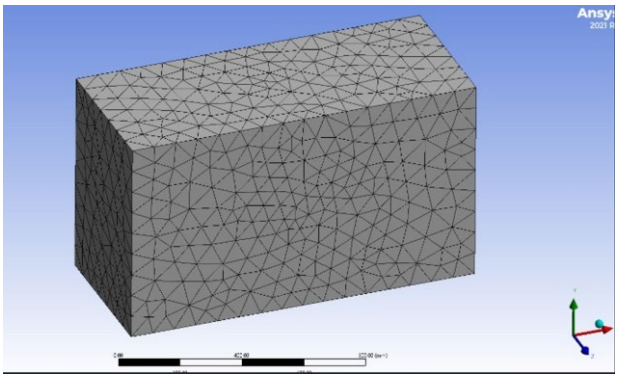

Fig. 5: Meshing.

The thermal analysis and the CFD yielded the following results. The following are the final ANSYS Fluent, and ANSYS Mechanical results are shown in Fig. 6 and Fig. 7. After iterations, the CFD solution converges.

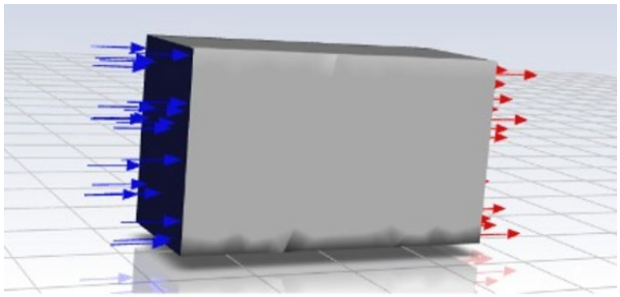

Fig. 6: Inlet of air.

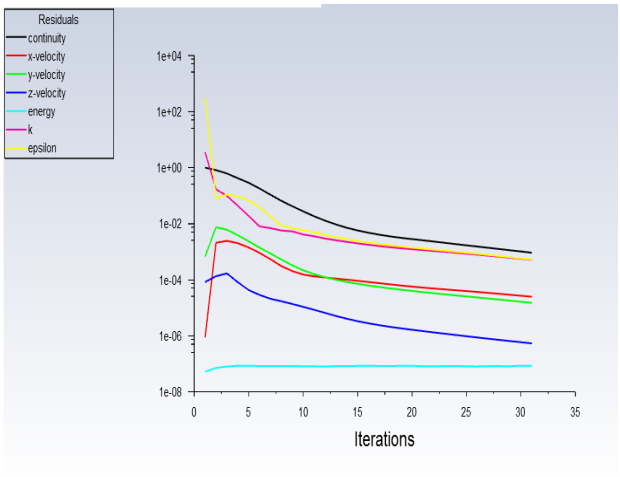

Fig. 7: Velocity distribution of disc.

The initial step in this research was to determine the interface temperature from the disc & pad. The disc was examined using the CFD program Ansys Fluent to accomplish this.

The study is heavily reliant on mesh quality. Fluent incorrect meshes cannot be analyzed in the analysis program. In Fig. 4 and Fig. 6, two different reference frames are adopted to treat the domain and the inlet of air, respectively. Before each analysis, the mesh quality was examined and determined to be suitable for the study. The mesh obtained had an orthogonal rate that was within the required criteria. The deviation in the shape of the mesh from its equilateral form is described by its skewness. Mesh should be designed as equilateral as possible. When considering a quadrilateral mesh, the angle of an equilateral mesh is 90 degrees, and the rise of a triangular mesh is 60 degrees. The less accurate the answer is, the more deviations from the equilateral mesh shape their maximum permitted skewness ratio is 0.95, and the average skewness might be as low as 0.33. The worst cells' orthogonal quality will be closer to 0, while the most excellent ones will be closer to 1. The minimum orthogonal rate for all cells should be more than 0.01, with a significantly higher average value. As indicated in

Table 5, the CFD parameters are as follows:

Table 5. CFD parameters.

Parameter	Inputs
Solver type	pressure based
Model used	k-ε, standard
References values	computed from inlet
Fluid used	Air (incompressible ideal gas)
Moderate load	20 N to 80 N
Pressure outlet	1 atm

Fig. 8 depicts the flow chart analysis of the experimental & analytical methodology for the interface temperature of the disc brake using CFD. This solution can be used to calculate the temperatures at which the disc and pad interfaces attain during uniform deceleration braking. This can be used to calculate the mass and heat transfer coefficient to the brake disc using Navier-Stokes and energy equation. The interface temperature of disc and pad has been experimentally measured with the help of infrared temperature sensor. Equivalent Von-Mises thermal stress was calculated by using CFD at constant temperature. The ventilated disc's cooling performance influences its mechanical function in the form of thermal stress and residual thermal stresses. Thermal analysis and investigation of the effects of the aforementioned parameters on the thermo-mechanical properties of the brake disc are the study's future works.

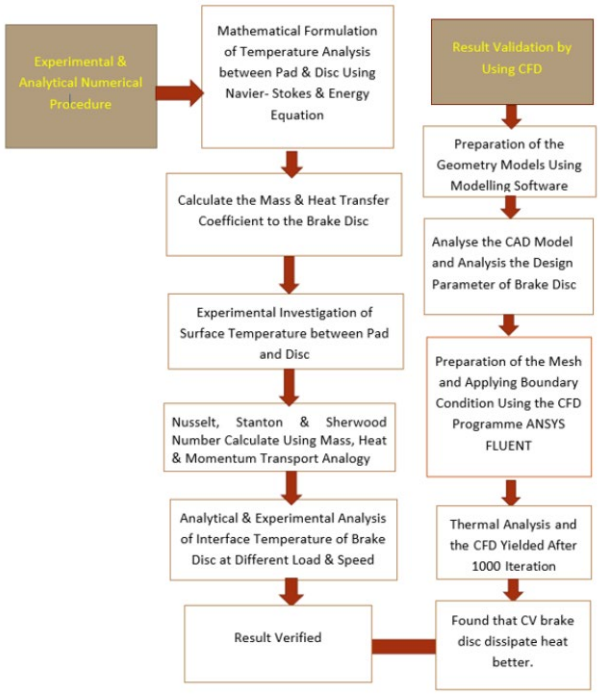

Fig. 8: Flow chart diagram of the experimental & analytical methodology for the interface temperature of the disc brake using CFD.

5. Experimental estimation of interface temperature between pad and disc

In the developed setup, power is transferred to the rotor under test via a generated flexible coupling, and as a prime mover, a suitable capacity A. C. motor is used. The rotor assembly is held between two plumber/bearing blocks, in continuation with the brake knuckle holding assembly shaft again this knuckle assembly is held between two Plummer / bearing blocks. Brake caliper assembly is mounted on knuckle assembly.

To apply load or Torque on the brake rotor, friction mechanism is used for good quality brake lining pads that are fitted between rotor and caliper assembly. Hand operated hydraulic pump is mounted on main base frame and its fluid pressure line is connected to caliper cylinder.

The frictional material wear can directly affect the safety and braking performance in Fig. 9 wear rate N-80 N for constant sliding distance. The experimental procedure was repeated for different sliding speeds up to 1100 rpm, and the combinations of other testing parameters were presented in Table-1. The disc temperature of the interface was accurately measured using the thermal camera and infrared sensor. Variations in pressure at the braking pads were assessed with the aid of a pressure transducer. By measuring the distance between disc and pad contact, the brake pad's deterioration friction material was evaluated using a digital vernier caliper.

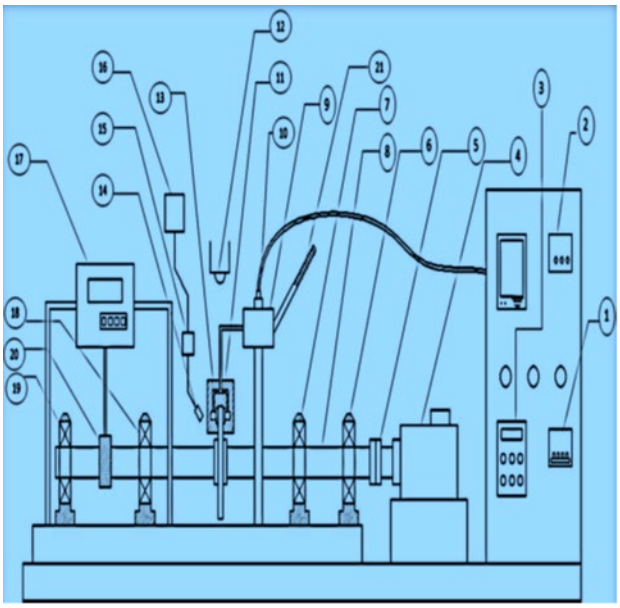

Fig. 9: Schematic diagram of developed test rig.

(1) Power Supply, (2) Pressure Display, (3) Variable Frequency Drive (VFD), (4) AC motor-3.7 kW, (5) Coupling, (6) (7) (18) (19) Bearings, (8) Main Shaft, (9) Hydraulic Oil Reservoir (10) Pressure Sensor, (11) Brake Calliper, (12) Infrared Camera, (13) Brake pads and Disc Mounting Unit, (14) Infrared Temperature Sensor, (15) Data Acquisition System (DAQ), (16) Computer Display, (17) Load Cell, (20) Loading Arrangement, (21) Lever.

5.1 Test procedure

The test rig comprises sensors like pressure, temperature, load cell along with the assembly of braking system; for maintaining speed and pressure constant VFD is incorporated, the pressure pump is used to maintain the pressure constant which may increase due to increase in temperature. The present system is compact, cheap and flexible as compared to other reported test rigs so far. The interface temperature of disc and pad is measured with the infrared temperature sensor. The temperature variation is the impact of different operating conditions. The brake test rig was used to investigate the pad friction material behavior at high speed (up to 1100 rpm) and moderate load (up to 80 N), and constant sliding distance (1000 m).

The wear test was started at ambient temperature and humidity under the dry condition with constant speed (300 rpm), and loads varied from 20 N. The equivalent von- Misses thermal stress at the disc brake varies from 0.041208 MPa to 347 MPa in Fig. 10.

6. Results & Discussion

The steady-state thermal stress at temperature and static structural factor in Fig. 10 and Fig. 11 represents that disc is dependent on the air velocity and also the air flow circulation in the disc. Thus the geometry that enables interface temperature at 550 rpm in 92°C will have better heat transfer characteristics and will ensure a more uniform temperature distribution. On visual inspection of temperature distribution for various geometries with holes drilled on their surface have better circulation of air and thus enabling uniform static structural safety factor.

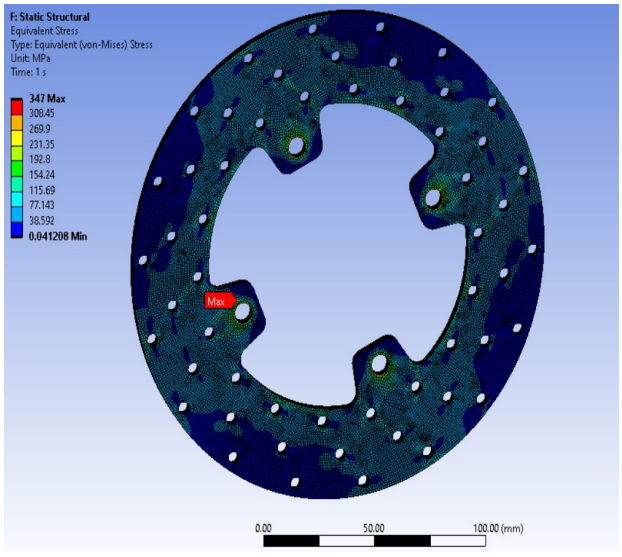

Fig. 10: Equivalent Von-Mises stress.

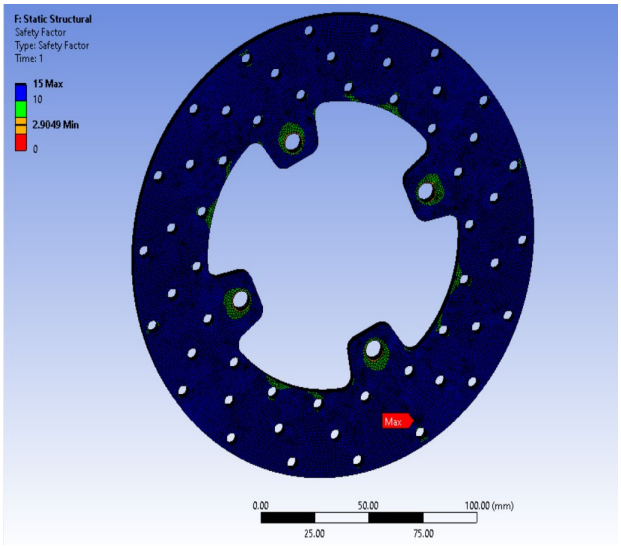

Fig. 11: Static structural safety factor.

The grid independence test is a process used to find the optimal grid condition that has the smallest number of grids without generating a difference in the numerical results based on evaluation various grid conditions. The grid independence test is used to determine whether the solution is dependent on mesh size. It shows in Fig. 12 us the limit till which we must refine our mesh to get accurate results, since further refining the mesh would only increase computation time.

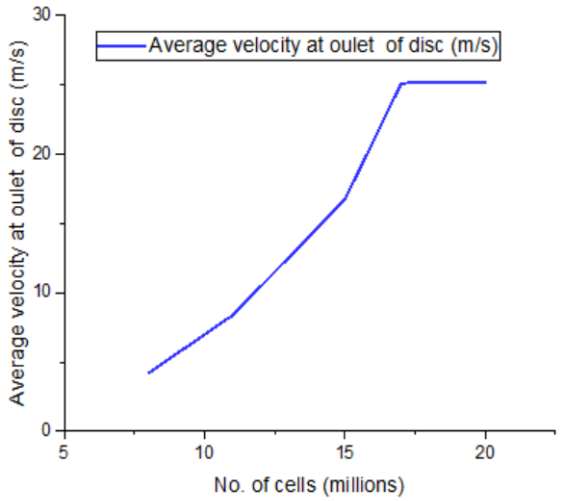

Fig. 12: Grid independence test of no. of cells vs average velocity at outlet of disc.

The wear rate under different brake operating conditions was tested, and experimental results are presented in Fig. 13. The brake pads were tested at other loads (20 N to 80 N), variable sliding speeds (300 rpm to 1100 rpm), different temperature change or temperature gradient (ΔT), and 1000 m constant sliding distance. The temperature at the interface between pad and disc varies from 82.1°C to 97.8°C as the speed varies from 300 rpm to 1100 rpm and loads from 20 N to 80 N. Variable frequency drive with panel mounted remote control used for motor speed control purpose. In addition, one can

adjust the motor's speed by rotating the VFD remote knob.

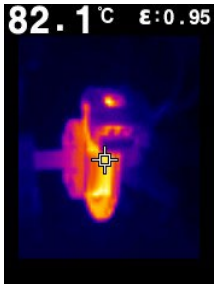

a: Interface temperature at 300 rpm

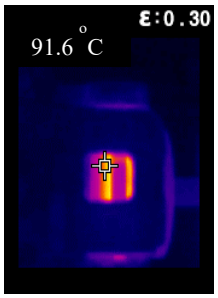

b: Interface temperature at 550 rpm

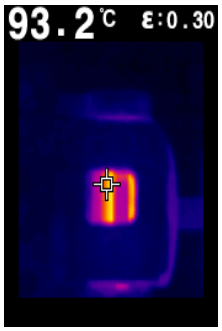

c: Interface temperature at 750 rpm

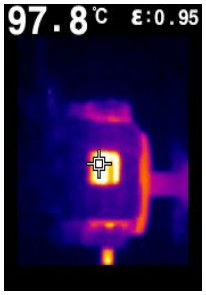

d: Interface temperature at 1100 rpm

Fig. 13 (a-d): Infrared thermal images of brake system for different speeds (300-1100 rpm) and different loads (20-80 N) at pad and disc.

This present study assumes a constant heat transfer coefficient to include the effect of varying heat transfer coefficients used to compute rotor temperature. At surface points, convective and radiation heat transfer was taken into consideration. The interface temperature between pad & disc is obtained from experimental results shown in Fig. 13. The interface temperature of disc and pad is measured with the infrared temperature sensor. The temperature variation is the impact of different operating conditions. As per earlier investigations the temperature can reach upto 100^0C for the disc brake interface without any heat resources resistant. The occurrence of automated driving offers a number of potential benefits, both on an individual and societal level, such as improved safety and fuel economy, increased heat dissipation, and reduced congestion problems, among other things.

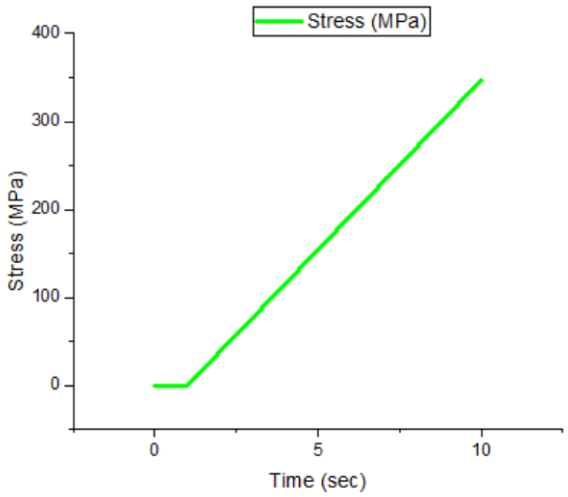

Fig. 14: CFD estimation of thermal stress at constant temperature.

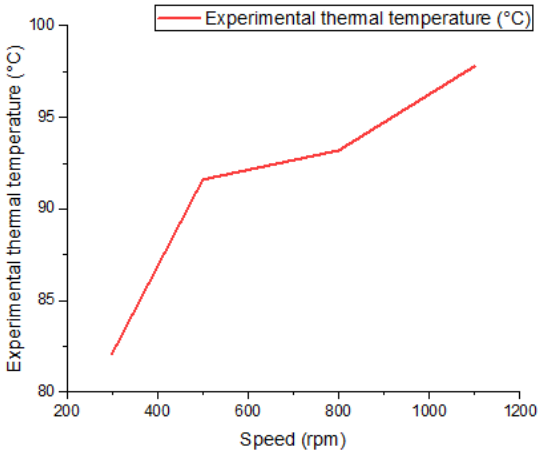

Fig. 15: Experimental estimation of interface temperature between pad & disc.

Equivalent Von- Mises thermal stress was calculated by using CFD in Fig. 14 and similarly calculated using an experimental brake test rig as shown in Fig. 15. Fig. 16 shows practical and theoretical results from equations (6) and (7) at various periods during single uniform brake applications at varying speeds. Each CFD point represents the average of at least four observations, with individual measurements having a scatter of 20-80 N around their mean. No forced air convection was

provided during the brake line when braking from an initial sliding surface. Instead, investigate the pad friction material behavior at high speed (up to 1100 rpm) and moderate load (up to 80 N), and constant sliding distance (1000 rpm). The wear test was started at ambient temperature and humidity under a dry condition with constant speed (300 rpm), and loads were varied from 20 N. Calculate the average value of the mass coefficients, and the local values must be integrated over the entire disc surface. Fig. 13 also shows the variation in average temperature rise for comparison. CFD was calculated using the agreement between thermal stress in Fig. 14 (0.0412 MPa to 347 MPa). The agreement between interface temperature between pad and disc in Fig. 15 shows the temperature at the pad-disc interface varies from 82.1°C to 97.8°C as the speed varies from 300 rpm to 1100 rpm, and the load varies from 20 N to 80 N was used to determine the experimental braking test rig. Fig. 14 shows experimental and theoretical findings from equations (6) and (8) at various times during single uniform brake applications at multiple speeds. Surprisingly, all the temperature rises in the first half of the study were within 5% of the theoretical estimated levels. Previous research focused on determining the thermal distortion and stress levels of a brake rotor, lowering the Von-Mises stresses and displacement vector sum and mass of the brake disc [48], increasing the velocity of mass movement through the passage [49], and calculating deformation and temperature.

The heat transfer measurements, as well as the numerical and experimental techniques used in this study, produced an average value of mass transfer coefficient, and heat transmission was consistent across the entire surface of a revolving disc in the regime of laminar flow. The solver results demonstrated that the proposed disc brake meets the favorable condition for the vehicle.

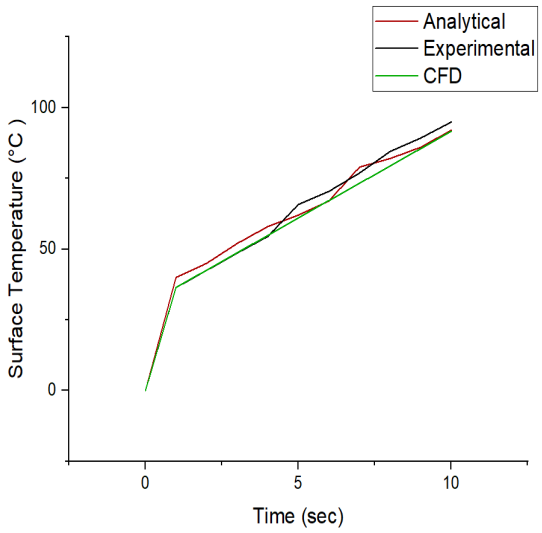

Fig. 16: Verification of interface temperature between pad & disc.

7. Conclusion

Computational flow dynamics is a valuable tool for analyzing and optimizing the cooling of disc brakes in passenger cars. The results obtained for the baseline and several modifications help gain a grasp of airflow into and out of the disc. The potential for disc cooling improvement can be determined, in particular, by examining alterations to a predetermined baseline. Many visualization types in certain places have been beneficial in comprehending the entire cooling air movement. For example, the steady-state thermal temperature was obtained from the ANSYS, and with the output from the CFD analysis, thermal analysis was performed in the ANSYS Mechanical. The heat transfer measurements and the numerical and experimental technique utilized in this study generated an average coefficient of transfer of mass, and heat transmission was consistent throughout the regime of laminar flow, the whole surface of a revolving disc. The results obtained from the solver demonstrated that the proposed disc brake is fulfilling the favorable condition for the vehicle. It is now possible to control air passage within the wheel housing. The experimental brake test rig was used to compute interface temperature between pad and disc and exhibits practical and theoretical results from equations (6) and (7) at various times during single uniform brake applications at multiple speeds. As the rate ranges from 300 rpm to 1100 rpm and the load varies from 20 N to 80 N, the temperature at the pad-disc interface varies from 82.1°C to 97.8°C. The thermal stress (0.0412 MPa to 347 MPa) were calculated using CFD. It can be evidenced that numerical and experimental studies enable to identify optimal heat dissipation for the brake system. This will be helpful to brake designers.

In addition to numerical simulation, mass and heat transfer coefficients from a rotating disc in an infinite environment under laminar and turbulent conditions can be calculated using Navier stokes and the energy equation. It was also analysed that the braking mode affected the disc brake's thermal behaviour. The numerical simulation shows that a number of parameters, including numerical parameters like the number of elements and the time phase, affect the consistency of the temperature field results.

Acknowledgements

Authors are thankful to Technical Education Quality Improvement Programme (TEQIP-III) at Veermata Jijabai Technological Institute (VJTI), Mumbai, India for financing the fabrication of experimental brake test rig.

Nomenclature

CFD	computational fluid dynamics
VFD	variable frequency drive

MFR	multiple future reference
FFT	fast fourier transform
BEM	boundary element method
m	total mass transfer rate in kg^{-1} sec
R_v	ideal gas of the vapour constant in J kg^{-1}°C
T_s	surface temperature of the disc in °C
$P_{v,s}$	pressure of the disc's vapours at T_s in Nm^{-2}
A	temperature of the disc's surface area in m^2
K_c	mass transfer coefficient in kg sec^{-1} m^2
η_r	recovery factor
C_p	specific heat
C_{Dr}	drag coefficient
d	brake drum or lining thickness
F	frictional force
h	coefficient of heat transfer
J	mechanical equivalent of heat
k	thermal conductivity
P	pressure.
r	internal radius of brake disc.
T	duration of brake application.
t	time
W	weight
V	linear speed at any instant
x	direction of heat flow
α	thermal diffusivity
μ	coefficient of friction
$\boldsymbol{\rho}$	density
β	angular displacement
ω	angular velocity
Nu	Nusselt number
Fo	Fourier number
Pr	Prandtl number

References

1) Belhocinea, A. R. Abu Bakarb, M. Bouchetaraa "Numerical modeling of disc brake system in frictional contact," *Tribology in Industry,* **36**(1), 49-66(2014).
2) C.H. Gao, X.Z. Lin, "Transient temperature field analysis of a brake in a non-axisymmetric three dimensional model," *J. Materials ProcessingTechnology*,**129**(1-3),513-517 (2002) .https://doi: 10.1016/S09240136(02)00622-2
3) Öztürk, F. Arslan, S. Öztürk, "Effects of different kinds of fibers on mechanical and tribological properties of brake friction materials," *Tribology Transactions*, **56**(4), 536-545(2013).https://doi:10.1080/10402004.2013.767399
4) S.P. Jung, T.W. Park, Y.G. Kim,"A study on thermal characteristic analysis and shape optimization of a ventilated Disc," *International Journal of Precision Engineering and Manufacturing,* **13** (1), 57-63 (2012). https://doi.org/10.1007/s12541-012-0008-4
5) O.I. Abdullah, J. Schlattmann,"Finite element analysis of temperature field in automotive dry friction clutch," *Tribology in Industry*, **34** (4), 206-216 (2012).
6) Anders Jerhamre and Christer Bergström," Numerical study of brake disc cooling accounting for both aerodynamic drag force and cooling efficiency," *SAE technical paper series*, Reprinted From: Brake Technology, ABS/TCS, and ControlledSuspensions,2001.https://doi.org/10.4271/2001-01-0948
7) Shen Z.F., Mukutmoni D., Thorington K. & Whaite J., Computational Flow Analysis of Brake Cooling, S A E Technical Paper 971039, 1997.
8) Owen J.M. & Rogers R.H., Flow and Heat Transfer in Rotating-Disc Systems, ISBN 0-86380-090-4, Research Studies Press Ltd., 1989.
9) Limpert, R. Cooling analysis of disc brake rotors. SAE paper 751014, 1975.
10) Newcomb, T. P. Thermal aspects of railway braking. Proc. Instn Mech. Engrs, Conference paper C154/79, 1979.
11) Fukano, A. and Matsui, H. Development of the disc-brake design method using computer simulation of heat phenomena. SAE paper 860634, 1986.
12) Belhocinea, A.R. Abu Bakarb, M. Bouchetaraa , Thermal and structural analysis of disc brake assembly during single stop braking event, Australian Journal of Mechanical Engineering, **36**(1), 2016:26-38. https://doi.org/10.1080/14484846.2015.1093213
13) S.V. Tsinopoulos, J.P. Agnantiaris, D. Polyzos, "An Advanced Boundary Element/Fast Fourier Transform Axis symmetric Formulation for Acoustic Radiation and Wave Scattering Problems", International Journal of Engineering Trend and Technology, vol. **105**, 1999: pp. 1517-1526.
14) Naga Phaneendrai, S. Junaid Razi , Wasee Ul Kareem, G. MD. Adnan & S. MD. Abdul Ahad, "Thermal Analysis of Solid Disc Brake Rotor", International Journal of Mechanical and Production Engineering Research and Development, Vol. **8**, pp. 1039-1048 (2018).
15) T. P. Newcomb, "Transient temperatures in brake drum and lining", *SAGE Journal of Automobile Engineering,* Vol.**7**, pp.227-244 (1958).https://doi.org/10.1243/PIME_AUTO_1958_000_028_02
16) Akiro Fukano and Hiromichi Matsui (Nissan Motor Co., Ltd.): "Development of Disc-Brake Method Using Computer Simulation of Heat Phenomena" in: *SAE Technical Paper* Series No. 860634, (1986).
17) R. K. Uyyuru, M. K. Surappa, and S. Brusethaug," Tribological behavior of Al–Si–Sic

composites/automobile brake pad system under dry sliding conditions," *Tribol. Int.,* **40** (2), pp. 365–373 (2007).https://doi:10.1007/s11249-011-9819-1

18) S.S. Kang and S.K. Cho," Thermal deformation and stress analysis of disk brakes by finite element method," *J. Mech. Sci. Technol*., **26** (7), pp.2133–2137 (2012)**.**https://doi:10.12691/ajme-2-4-2
19) L. Gudmand-Hoyer, A. Bach, G. T. Nielsen, and P. Morgen," Tribological properties of automotive disc brakes with solid lubricants," Wear, **232**(2), pp.168–175 (1999).
20) D. McPhee and D. A. Johnson," Experimental heat transfer and flow analysis of a vented brake rotor*, Int. J. Therm. Sci.,* vol. **47**,458–467 (2008). https://doi:10.1016/j.ijthermalsci.2007.03.006
21) L. Wallis, E. Leonardi, B. Milton, and P. Joseph,"Air flow and heat transfer in ventilated disc brake rotors with diamond and tear-drop pillars," *Numer. Heat Transf.* Part A Appl., vol. **41**, no. Issue 6–7, pp. 643–655 (2002). https://doi.org/10.1080/104077802317418269
22) Johnson, B. A. Sperandei, and R. Gilbert," Analysis of the flow through a vented automotive brake rotor," *J. Fluids Eng.,* **125** (6), pp. 979–986 (2003). https://doi:10.1007/s12239-013-0061-8
23) S. P. Jung, H. S. Song, T. W. Park, and W. S. Chung, "Numerical analysis of thermoelastic instability in disc brake system," *Appl. Mech. Mater.,* vol. **110**, pp. 2780–2785 (2012).
24) STAR-CD Manuals Version 2.2, Computational Dynamics Limited, London, (1993).
25) STAR-CD Manuals Version 2.2 Methodology - Part 2, Numerical Solution Techniques, Computational Dynamics Limited, London, (1993).
26) A.R. AbuBakar, H. Ouyang,"Complex eigen value analysis and dynamic transient analysis in predicting disc brake squeal," *Int. J Vehicle Noise Vib.* **2** (2), 143–155 (2006).https://doi. 10.1007/978-3-319-15236-3_10
27) S. James," An experimental study of disc brake squeal," Ph.D. Thesis, Department of Engineering, University of Liverpool, UK, (2000).
28) Naji M, Al-Nimr M, Masoud S,"Transient thermal behavior of a cylindrical brake system," *J Heat Mass Transf* **36**, 45–49 (2000). https://doi:10.1007/s002310050362
29) Mosleh M, Blau PJ, Dumitrescu D," Characteristics and morphology of wear particles from laboratory testing of disk brake materials," *J Wear* **256**,1128–1134 (2004). https://doi:10.1016/j.wear. 2003.07.007
30) Mutlu I, Alma MH, Basturk MA,"Preparation and characterization of brake linings from modified tannin-phenol formaldehyde resin and asbestos-free fillers," *J Mat Sci* **40**(11), 3003–3005 (2005).https://doi:10.1007/s10853-005-2396-7
31) Hecht RL, Dinwiddie RB, Wang H," The effect of graphite flake morphology on the thermal diffusivity of gray cast irons used for automotive brake discs," *J Mat Sci* **34** (19),4775–4781 (1999).https://doi:10.1023/A:1004643322951
32) Gudmand-Hyer L, Bach A, Nielsen GT, Morgen P," Tribological properties of automotive disc brakes with solid lubricants," *J Wear* **232**(2), 168–175 (1999).https://doi:10.1016/S0043-1648(99) 00142-8
33) Uyyuru RK, Surappa MK, Brusethaug S," Tribological behavior of Al–Si–SiCp composites/automobile brake pad system under dry sliding conditions". *J Tribol Int* **40**(2), 365–373 (2007). https://doi:10.1016/j.triboint.2005.10.012
34) Cho MH, Cho KH, Kim SJ, Kim DH, Jang H," The role of transfer layers on friction characteristics in the sliding interface between friction materials against gray iron brake disks", *Trib Lett* **20**(2), 101–108 (2005). https://doi:10.1007/s11249-005-8299-6
35) Boz M, Kurt A," The effect of Al2O3 on the friction performance of automotive brake friction materials," *J Tribo Int* **40**(7), 1161–1169 (2007). https://doi: 10.1016/j.triboint.2006.12.004
36) Blau PJ, McLaughlin JC," Effects of water films and sliding speed on the frictional behavior of truck disc brake material" ,*Trib Int.* **36**(10), 709–715 (2003). https://**doi:** 10.1016/S0301-679X(03)00026-4
37) Gao CH, Lin XZ,"Transient temperature field analysis of a brake in a non-axisymmetric three-dimensional model"*, J Mat Proc Tech* **129**, 513–517(2002). https://doi:10.1016/S0924-0136(02)00622-2
38) Jiusheng, Bao, Zhu Zhencai, Yin Yan, and Chen Guoan. "Influence of initial braking velocity and braking frequency on tribological performance of non-asbestos brake shoe*", Industrial Lubrication and Tribology* **61**,pp. 332–338 (2009). https://doi.org/10.1108/00368790910988453
39) Kumar Anil, Giri Rakesh, Mishra Shivnath, Gupta Niraj," Productivity improvement of HLLS using lean technique in assembly line of an automotive industry", *Evergreen-Joint Journal of Novel Carbon Resource Sciences & Green Asia Strategy,* vol.**9**, issue2, 356-366, (2022). https://doi.org/10.5109/4794160
40) Shashi Prakash Dwivedi, Maurya Manish, Shailendra Singh Chauhan," Mechanical, Physical and Thermal behaviour of SiC and MgO Reinforced Aluminium based composite material", *Evergreen-Joint Journal of Novel Carbon Resource Sciences & Green Asia Strategy,* vol.**8**, issue2, 318-327 (2021). https://doi.org/10.5109/4480709
41) N.I. Ismail, Shrudin Hazim, Mahadzir M. M, Zurriati M. Ali," Computational Aerodynamics Study on Neo-Ptero Micro Unmanned Aerial Vehicle", *Evergreen-Joint Journal of Novel Carbon Resource Sciences & Green Asia Strategy,* vol.**8**,issue2, 438-444 (2022).https://doi.org/10.5109/44807726

42) Stevens K, Leiter R, Taylor M, "Thermal Aspects in Electronic Parking Braking of Commercial Vehicles", In: *European Conference on Braking*, Lille, France, 2010.
43) S. Saedodina , M. J. Noroozi, D. D. Ganjib "Investigation of the Effects of Non-linear and Non-homogeneous Non-Fourier Heat Conduction Equations on Temperature Distribution in a Semi-infinite Body", *International Journal of Engineering*, IJE TRANSACTIONS C: Aspects..Vol. **28**, No. 12, (December 2015) 1802-1807.
44) M.H. Shojaefard and M. Fazelpour, "Effect of contact pressure and frequency on contact heat transfer between exhaust valve and its seat", *IJE Transactions B*: Applications Vol. **21**, No. 4, (December 2008), 401-408.
45) Verma P. C., Rodica C., Andrea B., Pranesh A., Giovanni S., and Stefano G., "Role of the friction layer in the high-temperature pin-on-disc study of a brake material", *Wear* 346 (2016) 56-65.
46) Lee, Kwangjin, and J. R. Barber. "An experimental investigation of frictionally-excited thermoelastic instability in automotive disk brakes under a drag brake application", *Journal of Tribology* (1994) 409-414.
47) L. Augustins, F. Hild, R. Billardon, S. Boudevin "Experimental and numerical analysis of thermal striping in automotive brake discs" **,**Fatig. Fract. Eng. Mater. Struct., 40 (2017), 267-276.
48) Prashant Patel, M.A. Mohite, "Design optimization of passenger car front brake disc for improvement in thermal behavior, weight & Cost reduction", *International Journal of Engineering Development and Research*, Vol.**5**. Issue 2, (2017) 1079-1086.
49) Jimit G. Vyas, M. J. Zinzivadia, M. I. Kathadi, "Design and Analysis of Solid and Cross-Drilled Disc Brake Rotors", *International Conference on Research and Innovations in Science, Engineering & Technology*, Vol. **1**, (2017) 294-301.
50) Yuri Alexandrovich Kostikov, Alexander Mikhailovich Romanenkov "Approximation of the Multidimensional Optimal Control Problem for the Heat Equation (Applicable to Computational Fluid Dynamics (CFD))", Civil Engineering Journal 6(4), (2020) 743-768. DOI:10.28991/cej-2020-03091506